

MODELLING OF THE PEDESTAL GROWTH OF SILICON CRYSTALS

K. Surovovs^a, A. Kravtsov^b, and J. Virbulis^a

^a University of Latvia, Jelgavas iela 3, 1004 Riga, Latvia

^b KEPP EU, 5 Carnikavas Street, 1034 Riga, Latvia

Email: kirils.surovovs@lu.lv

Received 18 December 2020; accepted 13 May 2021

The pedestal method is an alternative to the well-known floating zone method, both of which are performed with high-frequency electromagnetic heating. Unlike the floating zone method, in the pedestal method a single crystal is pulled upwards from the melt. It allows one to lower feed rod quality requirements and simplify the process control due to the absence of open melting front. As the pedestal method has not been widely used in industry for silicon crystals, its development requires extensive numerical modelling. The present work describes application of the previously created mathematical model for crystals with diameters higher than it is currently possible in the experimental setup, as well as for the cone growth phase. Supplementary free surface heating, that prevents melt centre freezing during the seeding phase, has been added at the beginning of cone phase. After multiple sets of simulations, an optimal scheme of heating control for cone growth was proposed.

Keywords: single silicon crystal growth, numerical modelling, pedestal method

1. Introduction

1.1. Silicon crystals

Single silicon crystals have been widely used in industry for decades and are continuing to be demanded despite advances in research of other semiconductors. Resistivity of the grown crystal can be controlled by dopants that are added during the crystal growth. To enable precise resistivity control and successful operation of produced devices, the content of other impurities should be reduced to the lowest possible level.

To measure the impurity level in polycrystalline rods (e.g. with Fourier-transform infrared spectroscopy) they must be melted and recrystallized as single crystals. To ensure that the addition of dopants is as low as possible a crucible-free method, that eliminates liquid silicon contact with any other material, should be used.

1.2. Pedestal method

The pedestal method (PM), proposed in 1950s by Dash [1], is an alternative to the well-known

floating zone (FZ) method. In both methods, polycrystalline silicon rods are being melted by using a high-frequency (HF) electromagnetic one-turn inductor. The main difference between the two methods is that in PM the upper surface of polycrystalline rod is molten, thus the melt is situated on a silicon ‘pedestal’, and the single crystal is being pulled upwards from the melt (see Fig. 1, right). A complicated feature of the FZ method – an open melting front, i.e. a lower part of a feed rod where the silicon is being melted and flows downwards – is absent in PM. Therefore, feed rod quality requirements for PM can be lower (and the process control can be simpler) than in the FZ method [2].

PM has a limitation on an inductor shape in comparison with FZ that prohibits ‘needle-eye’ inductors: the diameter of the grown crystal cannot exceed the inner diameter of the inductor. It happens because in the cylindrical stage of crystal growth (when the shapes of the molten zone and the grown crystal diameter do not change) 11° meniscus angle (the angle between the free melt surface and the crystal side surface) is required [3], and the diameter of the molten zone cannot be smaller than the crystal diameter. Due to a large inductor

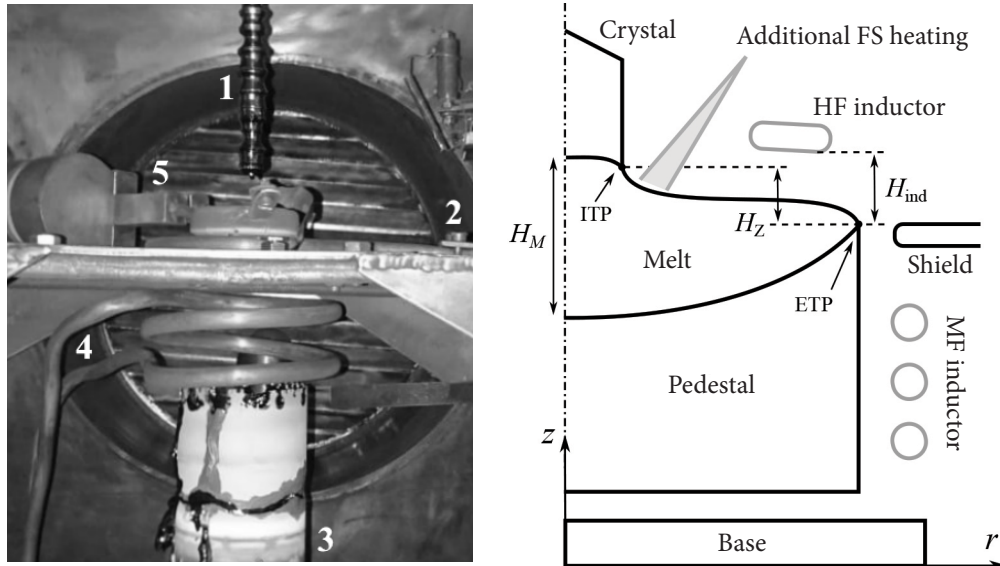


Fig. 1. Left: a growth chamber with a crystal seed (1), copper shield (2), pedestal (3), medium-frequency (MF) and HF inductors (4, 5). Right: a diagram of the modelled system.

diameter, freezing of the molten zone in the centre becomes more likely when the crystal diameter increases, and an additional medium-frequency (MF) inductor needs to be used for pedestal heating (see Fig. 1, left).

1.3. Numerical modelling

The experimental results are of limited quality and often do not provide an insight into all principal features of the growth process. To get this kind of information, numerical modelling is widely used. It allows one not only to reduce the number of expensive experiments, but also to supplement existing experiments by describing process features that are very hard to measure. Examples include distributions of various physical fields inside solid, melt and surrounding atmosphere: temperature, velocity,

electromagnetic field, phase boundaries, etc. Numerical modelling is particularly useful in the early development stages when parameter ranges of successful experiments are not known yet.

1.4. Aims of the study

The used inductor shape was optimized via the gradient method [4] to increase the melt height H_M for the cylindrical phase of a large (diameter $D_C = 100$ mm) crystal growth from the pedestal with a diameter of 200 mm. However, the experiments demonstrate [5] that at the seeding phase even the addition of a MF inductor is not enough to ensure that the free surface (FS) is completely molten (see Fig. 2). This difficulty arises because of large heat losses from the central part. It can be compensated by additional FS heating Q_{FS} , e.g.

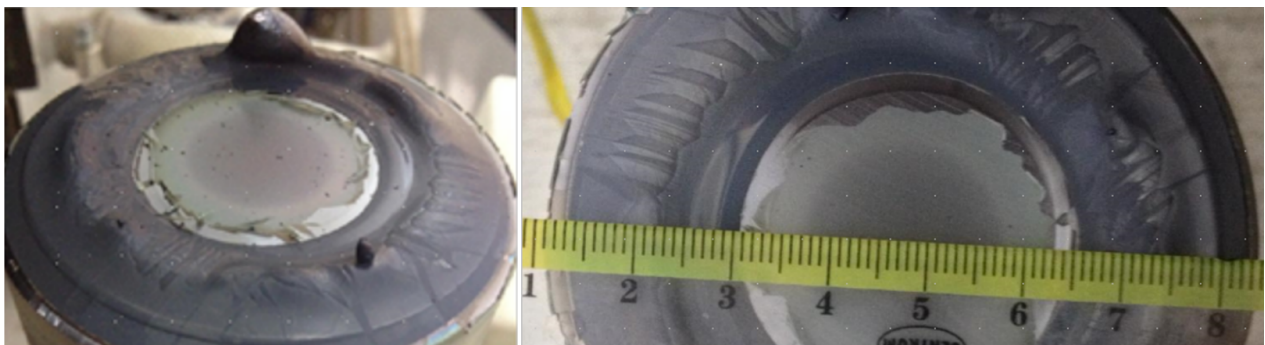


Fig. 2. Pedestal surface after unsuccessful attempts to melt it without additional FS heating.

with infrared lamps (schematically shown in Fig. 1, right).

The present work describes the calculations of phase boundaries for different crystal diameters, performed to find appropriate proportions of HF, MF and additional FS heating during the cone growth.

2. Modelled system

The used parameters are listed in Table 1. For a more detailed description of the growth apparatus see Ref. [5].

The MF inductor was made of a 10 mm copper tube and consisted of 3 turns, located approximately 10 mm from the pedestal side surface, as shown in Fig. 1. To separate MF and HF electromagnetic fields, a copper shield was installed between them.

3. Mathematical model

The shape of phase boundaries was obtained in the axially symmetrical approximation, using the previously developed software [6], based on the principles described in [7]. Melt flow has not been taken into account. To save computational time the growth of the crystal cone was approximated by running quasi-stationary simulation for different cone diameters.

To calculate the induced heat of the HF inductor, the high-frequency approximation, as given in [7], was used due to a relatively small skin layer depth ($\delta = 1.4$ mm for the frequency of 2.6 MHz). MF induced heat, however, cannot be approximated by surface heat density only, thus the vector potential \vec{A} was calculated in all volume domains,

$$\nabla \times \nabla \times \vec{A} = \mu_0 \sigma (-i\omega \vec{A}) + \mu_0 \vec{J}, \quad (1)$$

$$q = \frac{j^2}{2\sigma} = \frac{\sigma E^2}{2} = \frac{\sigma}{2} \omega^2 A^2, \quad (2)$$

where q , j , E and A are the magnitudes of induced heat density, current density, electric field and vector potential, respectively; $\mu_0 = 4\pi \cdot 10^{-7}$ H/m, $\omega = 2\pi f_{\text{MF}} = 6.3 \cdot 10^5$ Hz is angular frequency, \vec{J} is current density in the MF inductor and σ is the Si electric conductivity. Only the azimuthal component A_φ was taken into account due to axial symmetry (disregarding current suppliers). Boundary conditions were the following: $A_\varphi = 0$ on the axis and $\frac{\partial A_\varphi}{\partial n}$ on the outer boundaries of the domain.

MF induced heat calculation is coupled with the calculation of phase boundaries. After the quasi-stationary shape of phase boundaries has been reached, Q_{MF} is found as the integral power over all Si domains.

Table 1. Main parameters of the modelled system

Crystal diameter D_C	10–100 mm
Pedestal diameter D_P	200 mm
Crystal pulling rate v_p	2 mm/min
MF heating power Q_{MF}	8.6–9.4 kW
HF heating power Q_{HF}	9.0–10.0 kW
Free surface heating Q_{FS}	0–0.45 kW
MF inductor frequency f_{MF}	100 kHz
HF inductor frequency f_{HF}	2.8 MHz
Distance from MF inductor to HF inductor	33 mm
Distance from ETP to HF inductor H_{ind}	9 mm
Distance from ITP to FS heating region	5 mm
HF inductor parameters:	
internal diameter	122 mm
distance to ETP	11 mm
cross-section length	40 mm
cross-section inclination angle	3°
thickness	6 mm

4. Results

During the study, the inductor shape remained constant, and the inductor current was adjusted using a proportional-integral-derivative (PID) algorithm to keep the vertical distance to the external triple point (ETP) constant: $H_{ind} = 9$ mm (see

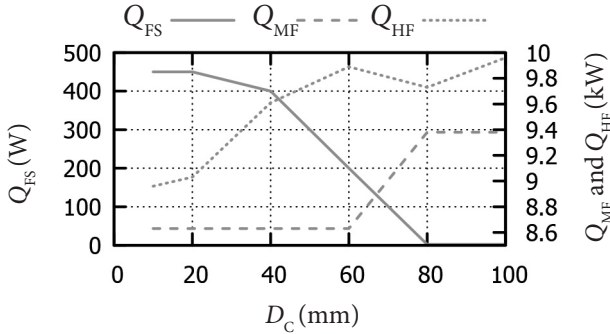


Fig. 3. The optimal values of integral free surface heat Q_{FS} , medium-frequency induced heat Q_{MF} and high-frequency induced heat Q_{HF} during the cone phase.

Fig. 1, right) for all of considered D_C . In this way, the total induced HF heat Q_{HF} has been obtained for each calculation. Other integral heat fluxes were user-defined. Q_{FS} was defined directly, Q_{MF} was defined indirectly – by defining MF inductor current. Multiple values were tested, and only some of calculations converged. For example, the melt centre was freezing when Q_{MF} was set too low, and part of FS crystallized near the internal triple point (ITP) if Q_{FS} was set too low. In this paper, the calculations with the lowest possible values of additional heat fluxes Q_{FS} and Q_{MF} are summarized, as they are beneficial for cost-effectiveness and equipment design. The optimized change of integral heat fluxes during the cone phase is given in Fig. 3, the corresponding phase boundaries and silicon temperature are presented in Fig. 4.

Both H_M value and FS shape are satisfactory, i.e. do not threaten a stable growth process, for all of crystal diameters except the largest

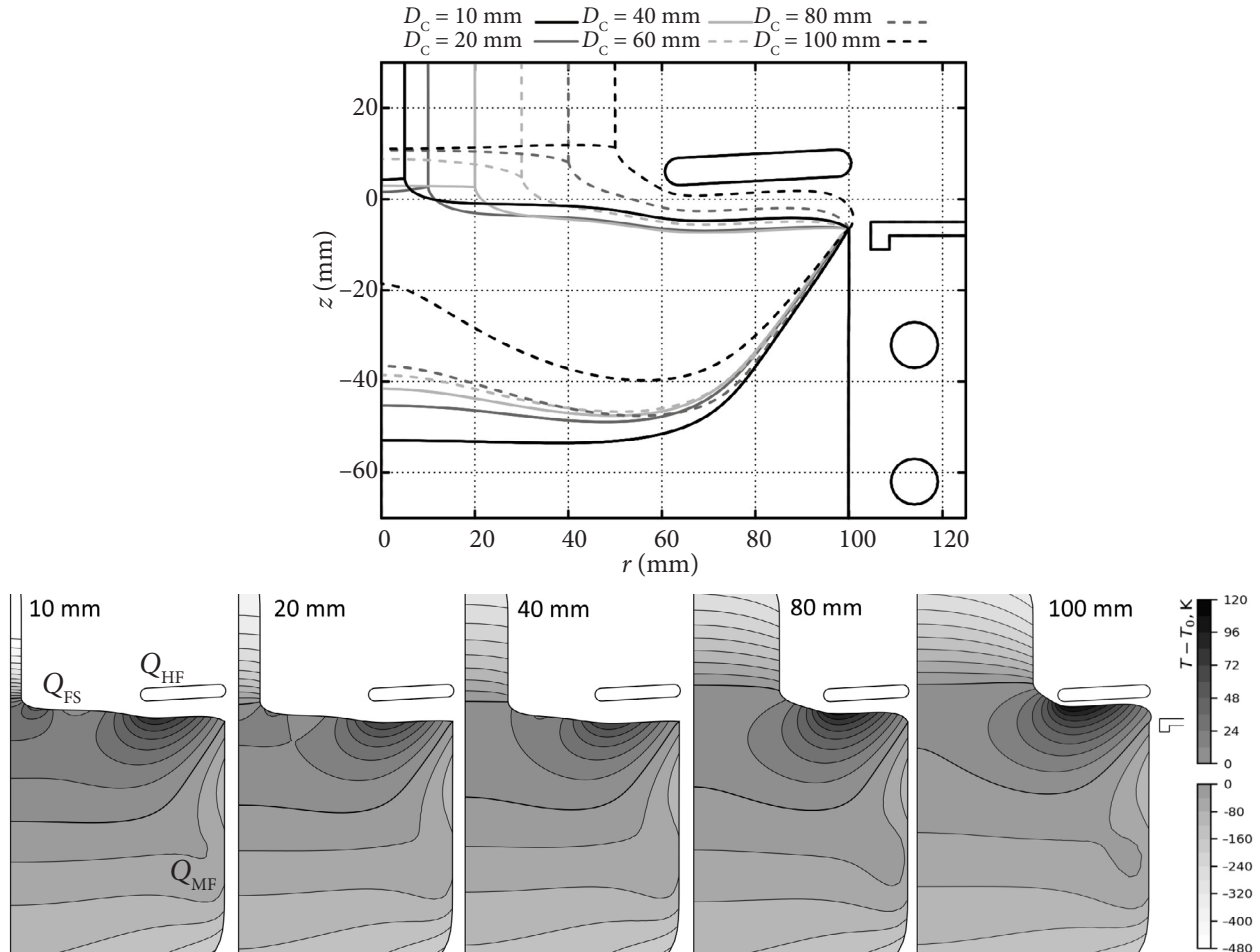


Fig. 4. Shapes of the phase boundaries (top) and corresponding silicon temperature (bottom) for different crystal diameters, with designation of heating regions Q (bottom left).

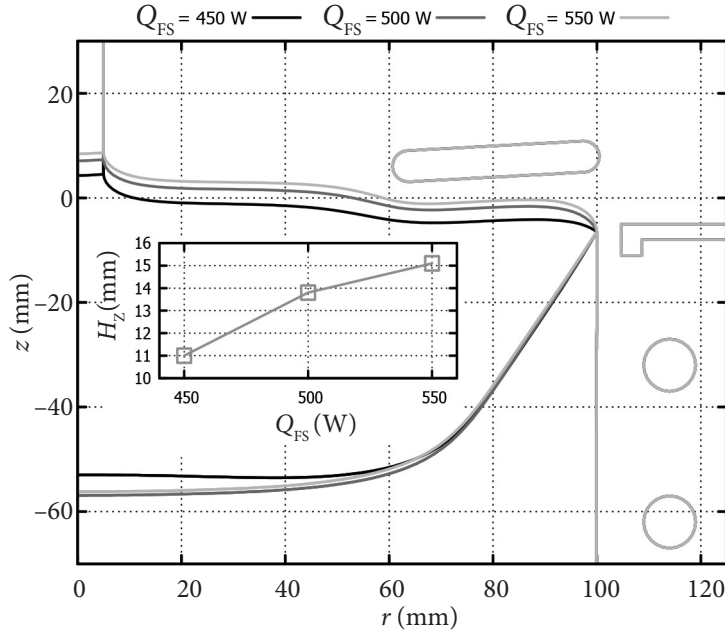


Fig. 5. Shapes of the phase boundaries (main graph) and the molten zone height (embedded graph) for the system with $D_c = 10$ mm and different additional free surface heat Q_{FS} .

$D_c = 100$ mm. In the latter case, FS is bulged outwards near the ETP, thus creating a high risk of melt spilling. We define α as the angle between the FS and the vertical line, with $\alpha > 0$ indicating that the surface goes ‘outwards’ from the ETP. Figure 4 shows that α is increasing when the induced heat in the vicinity of the crystal increases: either Q_{FS} (solid lines: from grey to black) or Q_{HF} (dashed lines: from grey to black). To illustrate this idea, Fig. 5 demonstrates the influence of Q_{FS} on the phase boundaries, while $D_c = 10$ mm and other parameters are constant. The embedded graph also shows the molten zone height H_z , defined as a vertical distance between the ETP and the ITP.

From Figs 4 and 5 it can be concluded that the increase of heat flux near the crystal shifts the ITP upwards, increasing the zone height, which increases α . This conclusion is affirmed by Fig. 6: when all considered D_c are summarized, a correlation between H_z and α is very strong. It means that to mitigate the risk of melt spilling over the ETP, the heat flux should be reduced in the vicinity of ITP.

A possible solution is to increase the inner diameter of the HF inductor. However, it would mean that induced heat is concentrated too close to the ETP, and low HF current will be sufficient to maintain the defined H_{ind} , which will increase the risk of melt centre freezing. The risk could be prevented by increasing the distance between the ETP and induced heat maximum, e.g. by increasing the pedestal diameter. It should also be noted that the currently used inductor shape has been optimized to improve only the melt height H_M , and another target function that includes α may be useful.

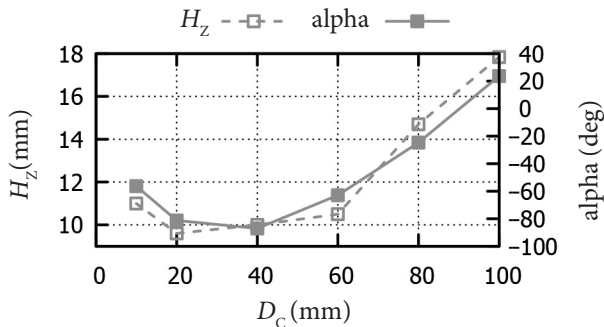


Fig. 6. Molten zone height H_z and the meniscus angle α at the ETP during the cone phase.

5. Conclusions

The performed calculations indicate that both MF and HF heating must increase during the cone phase, in order to a) compensate the decrease of

FS heating and b) compensate radiative heat losses from the crystal. The scheme of this increase is proposed in Fig. 3. The maximal FS heating, which is required for crystal diameters smaller than 20 mm, is less than 500 W.

The risk of melt spilling occurs only for the largest crystal diameter, i.e. in the cylindrical phase. To decrease the risk, the free surface angle could be improved by increasing the pedestal diameter or by modifying the target function in the inductor optimization method to take this angle into account.

Acknowledgements

The authors express their gratitude for the financial support provided by the European Regional Development Fund Project ‘Development of Competence Centre of Mechanical Engineering’, Contract No. 1.2.1.1/18/A/008, Research No. 4.5 ‘Technological Research and Silicon Production with Diameters up to 100 mm for Low-current and High-power Microelectronic Solid State Devices’.

References

- [1] W.C. Dash, Silicon crystals free of dislocations, *J. Appl. Phys.* **29**, 736 (1958).
- [2] W.C. Dash, Improvements on the pedestal method of growing silicon and germanium crystals, *J. Appl. Phys.* **31**, 736 (1960).
- [3] M. Wünscher, A. Lüdge, and H. Riemann, Growth angle and melt meniscus of the RF-heated floating zone in silicon crystal growth, *J. Cryst. Growth* **314**, 43–47 (2011).
- [4] K. Surovovs, A. Kravtsov, and J. Virbulis, Optimization of the shape of high-frequency inductor for the pedestal growth of silicon crystals, *Magnetohydrodynamics* **55**(3), 353–366 (2019).
- [5] A. Kravtsov, K. Surovovs, and J. Virbulis, Float zone single crystals for testing rods, pulled under electron beam heating, *IOP Conf. Ser. Mater. Sci. Eng.* **503**, 012022 (2019).
- [6] K. Surovovs, M. Plate, and J. Virbulis, Modelling of phase boundaries and melt flow in crucible-free silicon crystal growth using high-frequency heating, *Magnetohydrodynamics* **53**, 715–722 (2017).
- [7] G. Ratnieks, A. Muižnieks, and A. Mühlbauer, Modelling of phase boundaries for large industrial FZ silicon crystal growth with the needle-eye technique, *J. Cryst. Growth* **255**, 227–240 (2003).

SILICIO KRISTALŪ AUGINIMO PJEDESTALO BŪDU MODELIAVIMAS

K. Surovovs ^a, A. Kravtsov ^b, J. Virbulis ^a

^a *Latvijas universitetas, Ryga, Latvija*

^b *KEPP EU, Ryga, Latvija*